Available online at www.sciencedirect.com
ScienceDirect
Developmental Biology 309 (2007) 87–96
DEVELOPMENTAL BIOLOGY
www.elsevier.com/developmentalbiology

The Wilms tumor genes *wt1a* and *wt1b* control different steps during formation of the zebrafish pronephros

Birgit Perner [a], Christoph Englert [a,b,*], Frank Bollig [a]

[a] *Leibniz Institute for Age Research – Fritz Lipmann Institute, Beutenbergstrasse 11, 07745 Jena, Germany*
[b] *Friedrich-Schiller-University Jena, Germany*

Received for publication 23 March 2007; revised 13 June 2007; accepted 28 June 2007
Available online 3 July 2007

Abstract

The Wilms tumor protein WT1 is an essential factor for kidney development. In humans, mutations in *WT1* lead to Wilms tumor, a pediatric kidney cancer as well as to developmental anomalies concerning the urogenital tract. Inactivation of *Wt1* in mice causes multiple organ defects most notably agenesis of the kidneys. In zebrafish, two paralogous *wt1* genes exist, *wt1a* and *wt1b*. The *wt1* genes are expressed in a similar and overlapping but not identical pattern. Here, we have examined the role of both *wt1* genes in early kidney development employing a transgenic line with pronephros specific *GFP* expression and morpholino knockdown experiments. Inactivation of *wt1a* led to failure of glomerular differentiation and morphogenesis resulting in a rapidly expanding general body edema. In contrast, knockdown of *wt1b* was compatible with early glomerular development. After 48 h, however, *wt1b* morphant embryos developed cysts in the region of the glomeruli and tubules and subsequent pericardial edema at 4 days post-fertilization. Thus, our data suggest different functions for *wt1a* and *wt1b* in zebrafish nephrogenesis. While *wt1a* has a more fundamental and early role in pronephros development and is essential for the formation of glomerular structures, *wt1b* functions at later stages of nephrogenesis.

Keywords: Glomerulus; Tubule; Duct; Morpholino; Organogenesis; Kidney development; Podocyte

Introduction

In mammals three different excretory systems form during development. While the pronephros emerges most anteriorly and has no known function, the mesonephros arises more caudally and serves as the excretory organ of the embryo. The metanephros constitutes the definitive kidney and develops as the result of the interplay between two tissues, namely the nephric or Wolffian duct and the metanephrogenic mesenchyme. The former arises initially as the pronephric duct early in development and serves as the central component of the excretory system. The metanephrogenic mesenchyme induces the formation of an epithelial branch from each of the paired nephric ducts, the so-called ureteric buds. Subsequent reciprocal interactions between the ureteric buds and the kidney mesenchyme involving mesenchymal-to-epithelial transitions result in the formation of the glomeruli as well as the proximal and distal tubules of the nephron.

In teleost fish and in amphibians, the pronephros serves as the kidney of embryos and larvae. It consists of three components, namely the duct, the tubule and the glomerulus that develop in a stepwise fashion and in zebrafish begin to function as blood filter at 48 h post-fertilization (hpf) (Drummond et al., 1998). Concerning evolutionary conservation, it is interesting to note that transcription factors that are known to play a role in patterning the metanephric kidney in mammals do so also in the zebrafish pronephros. These are the product of the Wilms tumor suppressor gene *Wt1*, Pax2, a member of the paired-domain containing homeobox proteins as well as Sim-1, the vertebrate ortholog of the simple-minded transcription factor in *Drosophila*. Zebrafish *no isthmus* mutants (harboring mutations in *pax2.1*) display complete absence of pronephric tubules, whereas glomeruli and ducts remain intact (Majumdar et al., 2000). Mutants for zebrafish *sim1* and *wt1* have not yet been described. Although the metanephric kidney is much more complex than the pronephros, the latter harbors

* Corresponding author. Leibniz Institute for Age Research – Fritz Lipmann Institute, Beutenbergstrasse 11, 07745 Jena, Germany. Fax: +49 3641 656040.
E-mail address: cenglert@fli-leibniz.de (C. Englert).

0012-1606/$ - see front matter © 2007 Elsevier Inc. All rights reserved.
doi:10.1016/j.ydbio.2007.06.022

the same cell types as those that can be found in the metanephros, namely the endothelial cells of the capillaries, the mesangial cells and the podocytes (Drummond et al., 1998).

The podocytes are highly specialized cells that form the basis for blood filtration in the glomerulus (Pavenstadt et al., 2003). The actual filter is formed by slit diaphragms, particular cell junctions between the cell extensions of the podocytes, the so-called foot processes. Several molecules including the transmembrane protein Nephrin, the adaptor protein CD2AP, the protocadherin FAT, P-cadherin and Podocin contribute to the molecular structure of the slit diaphragm (Pavenstadt et al., 2003) or are thought to be required for its assembly (Huber et al., 2003; Roselli et al., 2004). The relevance of individual slit diaphragm components for the filtration process is underscored by the fact that mutations in the Nephrin as well as in the Podocin encoding genes cause nephrotic syndromes NPHS1 and NPHS2, respectively, in humans (Boute et al., 2000; Kestila et al., 1998). Interestingly, edema formation has also been reported for zebrafish *nephrin* and *podocin* morphants as well as for *mosaic eyes* mutant embryos (Kramer-Zucker et al., 2005b). As the respective proteins constitute components of the slit diaphragm, these observations extend the similarity of pronephros and metanephros to the function of components of the filtration barrier.

As mentioned above, the Wilms tumor suppressor Wt1 is a key regulator of kidney development. Inactivation of *WT1* in humans leads to Wilms tumor, a pediatric kidney cancer (Call et al., 1990; Gessler et al., 1990) as well as to other genitourinary malformations and dysfunctions (reviewed in Rivera and Haber, 2005). *Wt1* encodes a zinc-finger transcription factor and is expressed in various organs including the kidney, gonads and spleen (Armstrong et al., 1993; Pritchard-Jones et al., 1990; Rackley et al., 1993). In the developing kidney, *Wt1* mRNA levels are low in early stages and rise significantly as development proceeds. In the mature nephron, *Wt1* expression is confined to the podocytes (Armstrong et al., 1993; Pritchard-Jones et al., 1990). Resulting from usage of alternative translation initiation sites, RNA editing and alternative splicing, expression of *Wt1* results in various protein isoforms. The most prominent difference among the WT1 proteins is based on an alternative splicing event that leads to the insertion of three additional amino acids (KTS) between zinc fingers 3 and 4. Biochemical evidence suggests that the −KTS and +KTS isoforms of WT1 play different roles in transcription and RNA processing, respectively (Rivera and Haber, 2005).

In line with its expression pattern *Wt1* seems to have multiple roles during kidney development. In *Wt1*-knockout mice, the metanephrogenic mesenchyme is present at day 11.5 of embryonic development, ureteric buds, however, are absent (Kreidberg et al., 1993). Subsequently, apoptosis of the mesenchyme occurs and, half a day later, mesenchymal cells are no longer observed. Thus, in early kidney development Wt1 is directly or indirectly responsible for the generation of a signal from the mesenchyme that induces ureteric bud formation as well as for the competence of the mesenchyme to respond to signals from the ureter. In addition to this early function, there are indications that also suggest a late role for Wt1 in maintenance of kidney function. Patients with loss of one *WT1* allele (Riccardi et al., 1978) or with *WT1* point mutations (Barbaux et al., 1997; Klamt et al., 1998; Pelletier et al., 1991) show different signs of renal abnormalities. Moreover, mice with reduced or altered *Wt1* expression develop glomerulosclerosis and proteinuria (Guo et al., 2002; Lahiri et al., 2007). Interestingly, different *in vivo* functions for WT1(+KTS) and WT1(−KTS) have been demonstrated by the generation of respective mouse models (Hammes et al., 2001). Mice lacking the −KTS isoform show a severe kidney phenotype with a strong reduction of glomerulus number and size whereas mice deficient in the +KTS isoform have more subtle defects in glomerular structure and function.

In zebrafish knockdown of *wt1* leads to the formation of edema and suggests that wt1 is involved in the development of the pronephros (Hsu et al., 2003). Based on these observations an essential role of Wt1 in maintenance of podocyte function can be assumed. It is not clear what that role could be in molecular terms but the activation of podocyte-specific genes like *nephrin* (Guo et al., 2004; Wagner et al., 2004) and *podocalyxin* (Palmer et al., 2001) could contribute to it.

We have recently demonstrated the existence of a second *wt1* gene in zebrafish and have named the two genes *wt1a* and *wt1b* (Bollig et al., 2006). *Both* genes comprise 9 exons and the overall sequence identity of the two wt1 proteins is 70% and 92% between the zinc finger regions. Prompted by the differential temporal and spatial expression of *wt1a* and *wt1b* we wanted to address the role of both genes in the formation and function of the zebrafish pronephros. Using antisense morpholino oligonucleotides, we observed prominent pericardial and yolk sac edema formation in the case of *wt1a* while targeting of *wt1b* led to body curvature and to a more subtle edema formation that was restricted to the pericard. In addition, we have generated a transgenic zebrafish line that expresses *GFP* in the pronephric kidney. By using this line, we could show that inactivation of *wt1a* leads to the absence of glomeruli while targeting of *wt1b* resulted in the formation of renal cysts. These results provide evidence that the *wt1* genes play different functions during development of the pronephros in zebrafish.

Materials and methods

Maintenance of fish

Zebrafish embryos were obtained from matings of wild-type fish of the TüAB strain that has been kept in laboratory stocks in Würzburg and Jena for many generations. Embryos were raised at 28 °C and staged according to Kimmel et al. (1995).

Morpholino antisense oligonucleotides

Morpholino antisense oligonucleotides (GENE TOOLS, LLC, Philomath, OR, USA) were dissolved in water at a concentration of 3 mM. The stock solution was diluted to a working concentration of 1 mM in water with 0.1% phenol red (Sigma) and injected into the yolk of 1- to 4-cell embryos.

Oligonucleotides were designed which target the first splice donor site of both *wt1a* and *wt1b* pre-mRNAs (each called *splice1-1*). Additionally, a second oligonucleotide was used for both genes as an independent control, either blocking translation of the mRNA (*wt1a AUG*) or blocking usage of the second splice donor site (*wt1b-splice2-2*). As a standard control a morpholino was injected which targets a human *beta-globin* intron mutation. This morpholino has

not been reported to have any targets in zebrafish. The morpholino sequences are as follows: wt1a-splice1-1 AAA GTA GTT CCT CAC CTT GAT TCC T, wt1a-AUG CAC GAA CAT CAG AAC CCA TTT TGA G, wt1b-splice1-1 GGA TGG TTT TCT CAC CCT GGT TGC G, wt1b-splice2-2 CTC TAG TGT TCG TAC CCA TCG TCC T, control CCT CTT ACC TCA GTT ACA ATT TAT A.

A gradient of different injection volumes was tested for each morpholino in order to find the lowest morpholino amount, which leads to a consistent and reproducible phenotype. This amount was exactly determined for the *wt1a*- and *wt1b-splice 1-1* morpholinos by injection of ^{14}C labeled morpholino solutions. Radioactive counts of embryo lysates were measured in a scintillation counter and compared to the values of a standard dilution series. The average injection volume in our experiments was calculated to be 0.6 nl (0.6 pmol) for the *wt1a-splice 1-1* and 0.4 nl (0.4 pmol) for the *wt1b-splice 1-1* morpholino, respectively. The injection volume of the other morpholinos was estimated to be approximately 0.6 nl (0.6 pmol).

Conventional and quantitative real-time RT-PCR

Total RNA was isolated from zebrafish embryos using the RNeasy Mini Kit (Qiagen). Eluted RNA was subsequently treated with *DNase I* and reverse transcribed with SuperScript II RNase H$^-$ Reverse Transcriptase (Invitrogen) and oligo dT primers. To verify the absence of genomic DNA contamination, an aliquot of each RNA sample was used for PCR without reverse transcription. For conventional and quantitative real-time RT-PCR, the following primers were used: for *wt1a*, AGC CAA CCA AGG ATG TTC AG (exon 1 forward), CCT CGT GTT TGA AGG AGT GG (exon 2 reverse) and GAA TGC CAT TAA AGT AGT TCC TC (intron 1 reverse); for *wt1b*, TGC TGA TCC TCC TTC TAG CC (exon 1 forward), GAA CGG AGG AGT GTG TTG TG (exon 2 reverse) and GTC CTG AAT CAA CAA ATC CTT CC (intron 1 reverse); for *beta-actin*, GAG AAG ATC TGG CAT CAC ACC (forward) and AGC TTC TCC TTG ATG TCA CG (reverse).

For quantitative real-time RT-PCR, 1 μl of cDNA was used employing the QuantiTect SYBR green real-time PCR kit (Qiagen) on a Biorad iCycler in a 96-well format. All samples were measured as duplicates and normalized to the corresponding amounts of *beta-actin* cDNA measured within the same plate. Relative expression levels where calculated using the $2^{-\Delta\Delta CT}$ method (Livak and Schmittgen, 2001).

Generation of the transgenic wt1b:eGFP line

An arrayed zebrafish genomic P1 artificial chromosome (PAC) library (Amemiya and Zon, 1999) was obtained from the RZPD (German Resource Center for Genome Research, Berlin, Germany) and screened with a ^{32}P-labeled probe for *wt1b* exon 1, resulting in the isolation of 4 positive clones. Out of those, PAC clone BUSMP706A03157Q was used for subsequent cloning steps.

For construction of plasmid pBS-eGFP the cDNA of *enhancedGFP* (*eGFP*) was amplified from plasmid pEGFP-N1 (Clontech) using primer pair ACG TGG TAC CCA CCA TGG TGA GCA AGG G (forward) and ACG TGG TAC CAC AAC TAG AAT GCA GTG (reverse). The resulting PCR product (including *SV40* polyA signal) was cloned into the *Kpn*I site of pBSII-IsceI-SK+ (kindly provided by J. Wittbrodt, Heidelberg). This plasmid contains *I-Sce*I recognition sites, which enable efficient transgenesis in fish when the *I-Sce*I meganuclease is co-injected (Thermes et al., 2002).

In a second step, a 25.9-kb *Xho*I/*Apa*I genomic fragment was excised from zebrafish PAC clone BUSMP706A03157Q and ligated into the *Xho*I/*Apa*I sites of pBS-eGFP. The genomic fragment contains almost the entire region between *wt1b* and the 5′ neighboring gene *ga17*. It includes both the *wt1b* transcriptional and translational start site. The latter was removed by excision of a 184-bp *Eco*47III/*Apa*I fragment out of exon 1. In the resulting plasmid (named pBS-wt1b-eGFP) the *wt1b-eGFP* cassette is flanked by *I-Sce*I sites.

The pBS-wt1b-eGFP plasmid was co-injected with *I-Sce*I meganuclease (Thermes et al., 2002) in early one-cell stage zebrafish embryos (within 20 min after fertilization). The injection solution contained 150 ng/μl pBS-wt1b-eGFP plasmid, 0.4 U/μl *I-Sce*I meganuclease (Roche), 5 mM $MgCl_2$, 0.1% phenol red (Sigma) and 4 mM Tris–HCl pH 7.5.

Approximately 60 embryos injected with the pBS-wt1b-eGFP plasmid (F_0 generation) were raised to maturity and intercrossed. Offspring was analyzed for *eGFP* expression under a fluorescence stereomicroscope (SteREO Lumar.V12, Zeiss). GFP-positive embryos were isolated and raised establishing three stable transgenic lines (*wt1b*:eGFP 1-3).

Confocal fluorescence microscopy

Embryos treated with 1-phenyl-2-thiourea (PTU) and anesthetized with tricaine (0.016%) were embedded in 1% low melting point agarose (Biozym) with their back facing the bottom of a μ-dish (ibidi GmbH, München). For long-term imaging of living embryos, the agarose was overlaid with 0.3× Danieau's containing PTU and tricaine. For image acquisition, an ApoTome slider inserted into the reflected light beam of an inverted microscope was used (Axiovert 200, Zeiss). This set-up utilizes the principle of structured illumination to create optical sections. The recorded *z*-image stacks were assembled into projections with help of the AxioVision Inside 4D software (Zeiss).

Whole-mount in situ hybridization and histology

The cDNA fragment which was used for the riboprobe of zebrafish *podocin* (accession numberDQ466905) was amplified with primer pair CAA GAT CTG CCC GGA TAA AG (forward) and GCA GCT CTG GAG GAA GAT TG (reverse) giving rise to an 804-bp PCR product. The 796-bp cDNA fragment of zebrafish *nephrin* (accession numberNM_001040687) was amplified with primer pair GCG ATA CAG CAT GAC AGG AG (forward) and TTC AAA GGA GCC CAG TAA CG (reverse).

Whole-mount in situ hybridization was performed essentially as described (Hauptmann and Gerster, 1994). Embryos were hybridized with a digoxigenin labeled riboprobe of either *podocin* or *nephrin*. Anti-DIG AP and NBT/BCIP (Roche) were used to detect the probe. After color reaction, embryos were washed with methanol, equilibrated in clearing solution (1/3 benzoyl-alcohol and 2/3 benzoyl-benzoate) and photographed using a stereomicroscope (SteREO Discovery.V8, Zeiss). To suppress pigmentation, embryos were incubated with 0.003 % PTU. For hematoxylin–eosin (H&E) staining embryos were fixed in 3% PFA, washed in PBS and dehydrated in an ethanol series prior to embedding in paraffin. Sections of 4–6 μm were prepared and processed for routine H&E staining.

Results

Knockdown of wt1a and wt1b induces different phenotypes

In order to determine the function of the two paralogous *wt1* genes in zebrafish, we employed splice morpholinos, which bind to the first splice-donor site of *wt1a* and *wt1b*, respectively. This should lead to the inclusion of a 5.62-kb intron in the case of *wt1a* and of a 4.46-kb intron in the case of *wt1b* mRNA, resulting in premature in-frame stop codons in both cases. No PCR product could be amplified from cDNA of *wt1a* splice morpholino-injected embryos using a primer pair spanning exon 1 and exon 2 of *wt1a* (Fig. 1A, upper panel). In contrast, a strong signal was detected from the same cDNA when an intron 1-specific reverse primer was used confirming the inclusion of the first intron. In the same way the inclusion of the first *wt1b* intron after injection of the *wt1b* splice morpholino was confirmed (Fig. 1A, lower panel). Low amounts of unspliced RNA species could be observed also in control morpholino-injected embryos. These RNAs were more prevalent in the case of *wt1b*.

We used quantitative real-time RT-PCR (qRT-PCR) to quantify the reduction of correctly spliced mRNA and to monitor the time course of this effect (Fig. 1B). A dramatic reduction of *wt1a* and *wt1b* mRNA to 0.9% and 0.4%, respectively, was observed 1 day after injection although only

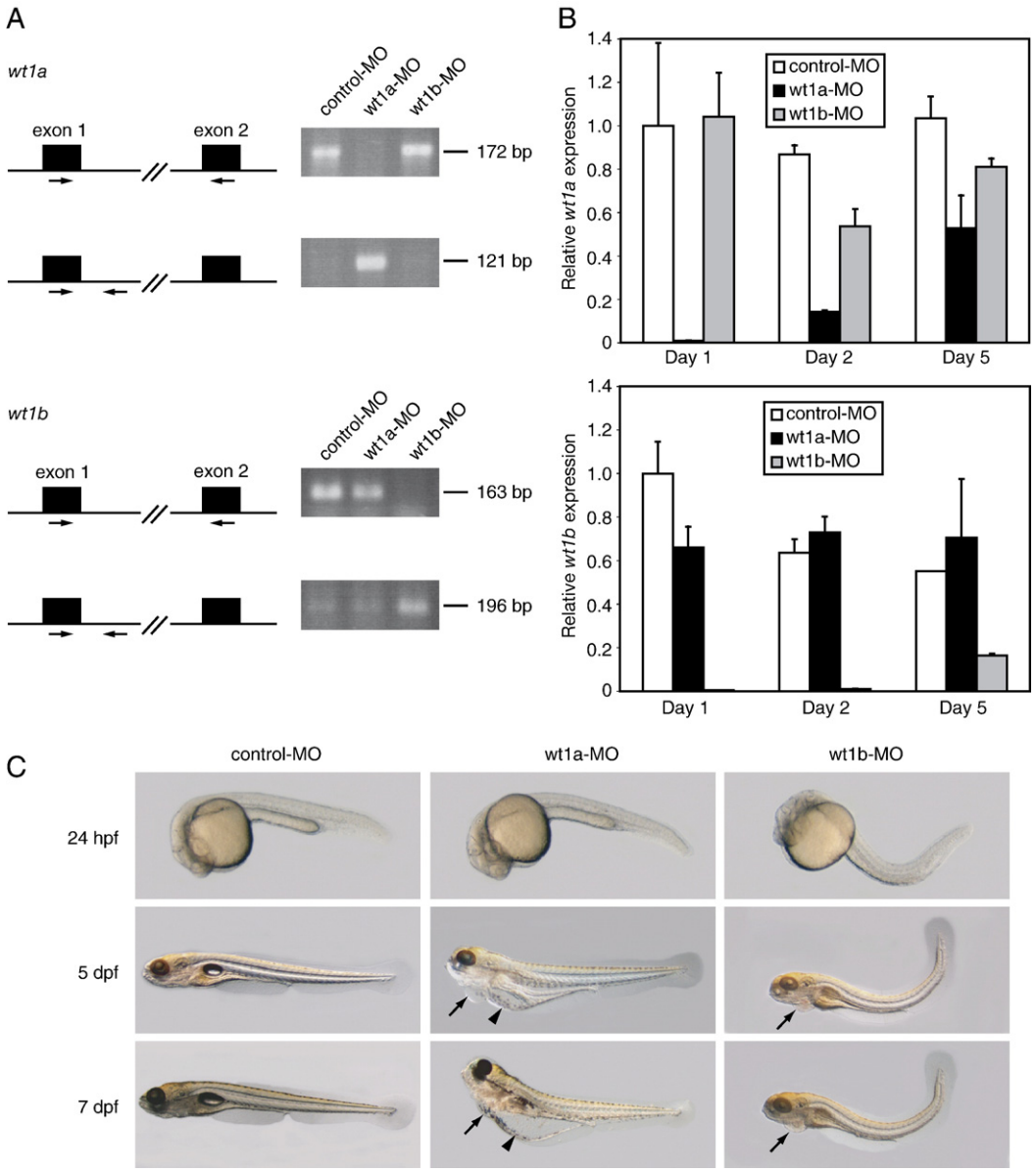

Fig. 1. Knockdown of *wt1a* and *wt1b* induces different phenotypes. (A) After injection of control, *wt1a* and *wt1b* morpholinos, RT-PCR analysis was performed from total RNA (10 pooled embryos from each injection). Both *wt1a* and *wt1b* primer pairs (indicated by arrows) are composed of a forward primer lying in the respective exon 1 and a reverse primer lying either in exon 2 (top panels) or in intron 1 (bottom panels). (B) Quantitative real-time RT-PCR was performed from total RNA of injected and pooled embryos at the indicated stage using primer pairs as described in panel A located in exon 1 and exon 2 of *wt1a* (upper panel) or *wt1b* (lower panel), respectively. All values were normalized to *beta-actin*. For comparison, expression in 1-day-old control embryos was set to 1. (C) Control, *wt1a* and *wt1b* morpholino-injected embryos are shown at different stages. Pericardial edema is marked by arrows and yolk sac edema by arrowheads; wt1a-MO, *wt1a* exon 1–intron 1 splice morpholino; wt1b-MO, *wt1b* exon 1–intron 1 splice morpholino; hpf, hours post-fertilization; dpf, days post-fertilization.

small amounts of splice morpholinos were injected (less than one picomole, see Materials and methods). *Wt1a* mRNA recovered faster (15% after two and 53% after 5 days) than *wt1b* mRNA (1% at day 2; 19% at day 5). This could be explained by higher expression levels of *wt1a* compared to *wt1b*. Importantly, morpholinos were specific and did not severely affect mRNA generation from the respective paralogous gene.

Wt1a morphant embryos did not show any phenotypic anomalies during the first three days post-fertilization (dpf). At day 4 knockdown of *wt1a* led to pericardial edema which subsequently developed into a more general edema after day 5 of development (Fig. 1C), as has been described (Hsu et al., 2003). Edemas were irreversible and led to death of the larvae presumably due to the inability to take up food. In contrast to *wt1a* morphants, disruption of *wt1b* mRNA resulted in body axis curvature that was already detectable at around 24 hpf. The direction and degree of curvature was variable, although the majority of *wt1b* morphant embryos showed a dorsally bent body axis (in some cases with a curled tail). After 4 days larvae that had been injected with a *wt1b* morpholino developed pericardial edema (Fig. 1C) but only a minority of them evolved general edema at 6 dpf or later (Table 1).

Table 1
Phenotypic alterations in *wt1a* and *wt1b* morpholino-injected embryos

Morpholino	*n* [a]	Curved body	Pericardial edema	Yolk sac edema
Control [b]	250	2 (<1%)	1 (<1%)	0
wt1a splice1-1	150	2 (1%)	141 (94%)	139 (93%)
wt1a AUG	94	1 (1%)	82 (87%)	69 (73%)
wt1b splice1-1	261	209 (80%)	189 (71%)	34 (13%)
wt1b splice2-2	92	73 (79%)	69 (75%)	14 (15%)
wt1a and wt1b splice1-1	135	109 (81%)	128 (95%)	127 (94%)

[a] *n*: number of injected embryos.
[b] This cohort comprises control morpholino injected and uninjected embryos. No phenotypic differences could be observed between these two groups.

We have attempted to rescue the defects associated with *wt1a* and *wt1b* knockdown by injection of capped *in vitro* transcribed *wt1a* or *wt1b* mRNA. However, the injection of even very small amounts of the respective mRNAs resulted in strong defects including formation of edema as well as anomalies in eye and forebrain development. This is probably due to alterations in the gene expression program associated with ectopic activity of a strong transcription factor like wt1a or wt1b and prevented us from using this approach.

To address the specificity of the effects observed, we have used additional morpholinos directed against different sequences within the *wt1a/b* RNAs. In the case of *wt1a*, an AUG morpholino and in the case of *wt1b* a morpholino directed against the second splice donor site has been used. In each case the same phenotypic changes could be observed as have been described above (Table 1 and Supplementary Fig. 1). Injection of a standard control morpholino did not induce any phenotypic alteration (Fig. 1C). Of note, all *wt1a* and *wt1b* morpholino-injected larvae showed a defect in inflation of the swim bladder. We cannot decide whether this effect is caused by edema formation or is due to a specific role of *wt1a* and *wt1b* in swim bladder formation. Generally, inflation of the swim bladder seems to be a process that is disturbed frequently in morpholino-injected embryos (Holtzinger and Evans, 2005; Kramer-Zucker et al., 2005b; Lang et al., 2006) as well as in naturally occurring mutants (McCune and Carlson, 2004).

After having demonstrated that inactivation of the two *wt1* genes leads to different phenotypic alterations, we wanted to explore the possibility that the two genes show some redundancy in their function. To this end, we have injected the splice morpholinos targeting the first splice donor site of *wt1a* and *wt1b* simultaneously. After 1 day, the embryos showed curvature of their body axis, followed by pericardial and yolk sac edema formation at day 4. These edema developed to a significant size after day 6 post-fertilization (Supplementary Fig. 2). No additional alterations in other organs or signs for attenuation or enhancement of the effects mediated by inactivation of either gene alone were seen. Thus, the phenotypic consequences of simultaneous inactivation of *wt1a* and *wt1b* correspond to the sum of the anomalies caused by disruption of either gene alone. At this level of analysis neither redundancy nor synergistic activity of the two *wt1* genes could be observed.

Generation of transgenic zebrafish lines with pronephros-specific GFP expression

In the zebrafish embryo, both *wt1* genes are most prominently expressed in the developing pronephros (Bollig et al., 2006). Moreover, the *wt1a* and *wt1b* morphant phenotypes that we observed resembled that of zebrafish mutants with kidney defects (Drummond et al., 1998; Sun et al., 2004). To examine the role of *wt1a* and *wt1b* during embryonic kidney development, we therefore sought to generate transgenic zebrafish lines with pronephros-specific *GFP* expression.

From a study in transgenic mice it could be concluded that elements responsible for *Wt1* expression in the mammalian kidney are located between *Wt1* and the 5′ neighboring gene *Ga17* (Moore et al., 1998). By bioinformatic analysis, we have found an ortholog of *Ga17* that is located approximately 28 kb upstream of *wt1b* in zebrafish and, as in mouse, is transcribed into the opposite direction (Fig. 2A). A *ga17* paralog could not be detected in the vicinity of *wt1a*. Since the upstream intergenic region of *wt1b* thus resembles the murine *Wt1* locus, we cloned a 25.9-kb fragment encompassing almost the entire region between *wt1b* and *ga17* (Fig. 2A). The fragment, which includes sequences from the 5′ UTR of *wt1b* but not the respective ATG, was fused to the gene encoding the *enhanced green fluorescent protein* (Fig. 2A). The resulting construct was injected in early one-cell stage embryos and 60 injected fish were raised to adulthood. Three positive founders were identified. All three produced offspring that showed *GFP* expression in the pronephric kidney. Each of the founders was used to establish an independent transgenic line (*wt1b:GFP 1-3*). For further analysis we used the *wt1b:GFP line 1* (hereafter named *wt1b:GFP*) because it exhibited the brightest *GFP* signal.

As judged by fluorescence microscopy, a GFP signal was first detectable in the pronephric region at 17 hpf in *wt1b:GFP* embryos (Fig. 2B). This is in agreement with the endogenous expression of *wt1b*, which can be detected at 15 hpf in the developing pronephros (Bollig et al., 2006). In 35 hpf embryos, *GFP* expression could be observed caudally to the second somite pair in an area that comprised the pronephric glomeruli, the pronephric tubules and proximal parts of the pronephric ducts (Fig. 2C). This was also confirmed by GFP *in situ* hybridization of transversal sections through the pronephric region (data not shown).

Starting approximately 30 hpf, *GFP* expression could be observed in putative progenitor cells of the exocrine pancreas (Figs. 2C, E) and later (65 hpf) also in the gut (Fig. 2E). As *wt1b* expression cannot be detected in these tissues, this expression can probably be attributed to enhancer elements of the 5′ neighboring gene *ga17*, which is expressed in endodermal tissues as shown by *in situ* hybridization on transversal sections (Fig. 2F). A weak GFP signal could be found in the developing heart sac, eyes and gill arches (Fig. 2D). In line with those observations, we have detected *wt1b* mRNA in the heart region of 3-day-old zebrafish larvae (data not shown) and in the heart, eyes and gills of adult zebrafish (Bollig et al., 2006).

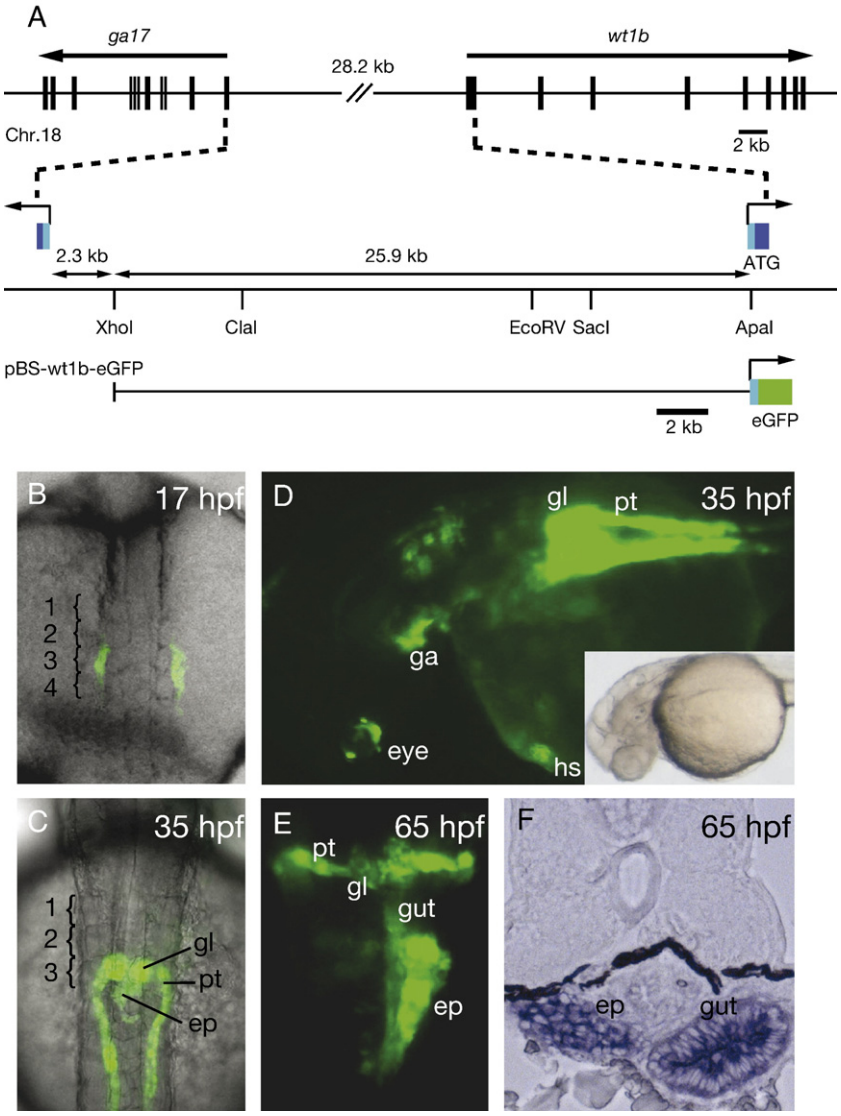

Fig. 2. Generation and characterization of a transgenic zebrafish line with pronephros-specific GFP expression. (A) Structure of the *wt1b* genomic region and the reporter construct. The upper panel shows the *wt1b* gene (9 exons) and the *ga17* gene (11 exons) lying on chromosome 18. 5′ to 3′ orientation of both genes is indicated. Exons are represented by black boxes. The middle panel shows a restriction map of the region between *ga17* and *wt1b* including the first exon of both genes. Untranslated regions are shown in light blue and coding regions in dark blue. Lower panel shows a schematic diagram of the construct used to generate transgenic fish. This construct contains an *XhoI*/*Apa*I genomic fragment fused to *eGFP*. (B, C) Overlays of transmission (gray) and fluorescence (green) dorsal images of 17 hpf (B) and 35 hpf (C) embryos, respectively. First four somites in panel B and first three somites in panel C are numbered and marked by parentheses; gl, glomerulus; pt, pronephric tubule; ep, exocrine pancreas. (D, E) Dorsolateral (D) and dorsal (E) fluorescence images of 35 hpf (D) and 65 hpf (E) embryos, respectively. The inset in panel D shows a bright-field image to illustrate the orientation of the embryo. Note that the image in panel D is overexposed with regard to the pronephros in order to display the weaker *GFP* expression in the eye, gill arches (ga) and the heart sac (hs). (F) A cross-section of a 65-hpf embryo through the middle of the yolk region is shown that has been hybridized with a *ga17* riboprobe.

Taken together, *GFP* expression in the *wt1b*:*GFP* line recapitulates to a large extent the expression of endogenous *wt1b*, particularly within the developing kidney. Thus, this line provides an ideal tool for studying kidney development *in vivo*.

Knockdown of wt1a and wt1b causes different defects during pronephros development

After having established a stable transgenic line with pronephros-specific *GFP* expression, we wanted to examine the consequences of *wt1a* and *wt1b* knockdown on early kidney development. To this end we have injected the *wt1a*- and *wt1b*-specific splice morpholinos into the *wt1b*:*GFP* line and have performed confocal microscopy at different time points.

In uninjected control embryos two pronephric ducts with nephron primordia at their anterior tips are visible at 24 hpf (Fig. 3A). Subsequently, the anterior parts of the pronephric primordia fuse at the midline. After 48 hpf the glomeruli have become functional blood filters (Drummond, 2003). At this time elaborate glomerular structures, the tubules that extend laterally as well as the ducts can clearly be distinguished in confocal images (Fig. 3A).

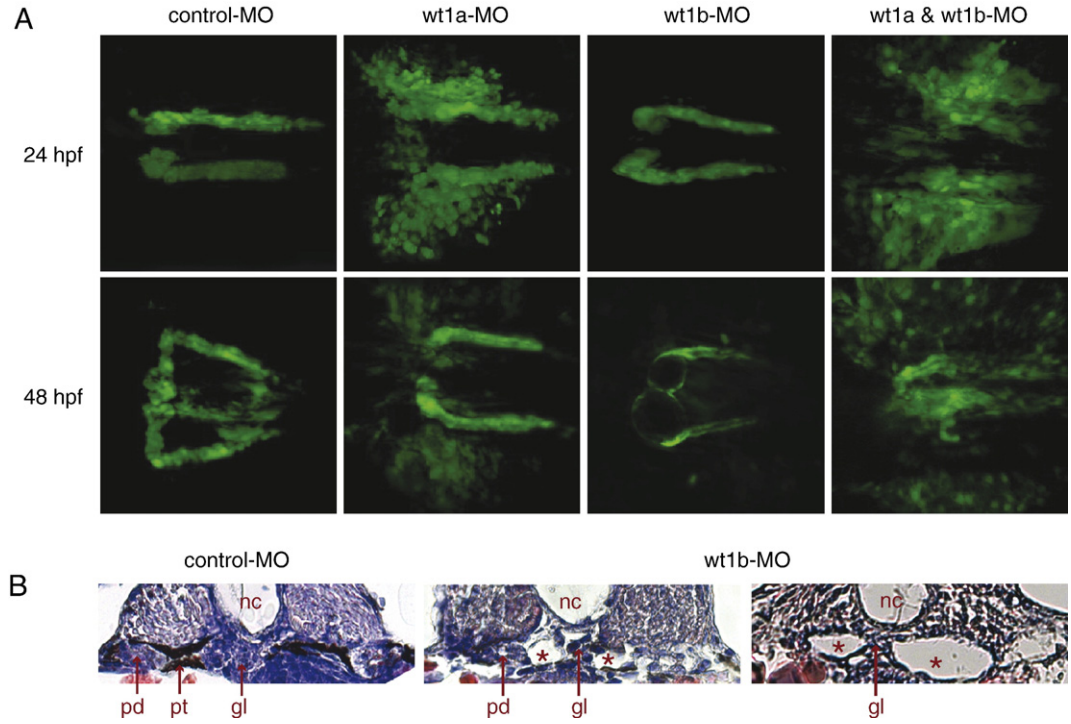

Fig. 3. Knockdown of *wt1a* and *wt1b* leads to different defects during pronephros development. (A) Confocal images of control and *wt1* morpholino-injected *wt1b:GFP* embryos were recorded 24 and 48 h after fertilization and assembled into 3D projections. (B) Formation of kidney cysts (asterisks) in *wt1b* morpholino-injected embryos 48 h after fertilization was visualized by H&E staining on cross sections. Note that a part of the glomerular filtration unit was still detectable between the cystic structures. *nc*, notochord; *gl*, glomerulus; *pt*, pronephric tubule; *pd*, pronephric duct.

Wt1a knockdown resulted in failure of glomerular morphogenesis. The GFP-positive duct structures were, however, unaltered. At 24 hpf, a large amount of GFP-positive cells were found to be outside of the pronephric field and no proper nephron primordia were formed (Fig. 3A). At 48 hpf, the most anterior part of the GFP-positive structures were slightly thickened and had moved towards the midline, but had not fused. Neither glomerular structures nor pronephric tubules were visible. Also at this time point a significant number of GFP expressing cells could be detected outside of the developing pronephros.

In contrast, during the first 24 h post-fertilization no obvious differences in pronephros patterning between control and *wt1b* knockdown embryos were observed. At 48 hpf, however, in around 70% of the injected embryos (99 embryos were examined in 3 independent experiments) cystic structures located in the tubular–glomerular region were observed (Fig. 3A). The formation of cysts was also confirmed by histological analysis (Fig. 3B). The size of the cysts was variable and in some cases they developed only unilaterally. Both fluorescence microscopy and histological examination suggested that at least part of the glomerular filtration apparatus was still present between the cystic structures.

When we knocked down both *wt1* genes the effects on glomerular development were stronger than in either case alone. There were no signs of formation of glomeruli (Fig. 3A). Moreover, in most cases structures resembling pronephric tubules or the proximal parts of the pronephric ducts were missing.

Differential loss of podocyte-specific marker genes in wt1a/b morphant embryos

To examine whether podocyte differentiation was still occurring in *wt1a/b* morphant embryos, we performed *in situ* hybridization with riboprobes for *nephrin* and *podocin*. Both genes are specifically expressed in the podocytes of the pronephric glomerulus and are both essential for pronephros function (Kramer-Zucker et al., 2005b).

At 48 hpf control embryos displayed *podocin* as well as *nephrin* expression as two rounded patches that are located next to each other (Fig. 4, left), reflecting expression in the pronephric glomeruli, as previously described (Kramer-Zucker et al., 2005b). Knockdown of *wt1a* resulted in complete loss of expression of both marker genes (Fig. 4, middle). This indicates the absence of podocytes and is thus in agreement with our observation that glomerulogenesis in *wt1a* morphant embryos is completely blocked. In contrast, in *wt1b* knockdown embryos the expression of both marker genes was still present (Fig. 4, right). In comparison to control embryos, however, the area of expression was reduced and the pattern appeared more stripe-like. The clearly detectable expression indicates that podocyte differentiation has occurred within the nephron primordia. The results support our presumption that the filtration unit is at least in part present in *wt1b* morphant embryos.

The different effect of *wt1a* and *wt1b* knockdown on marker gene expression correlated well with the results from fluorescence microscopy and the severity of the observed

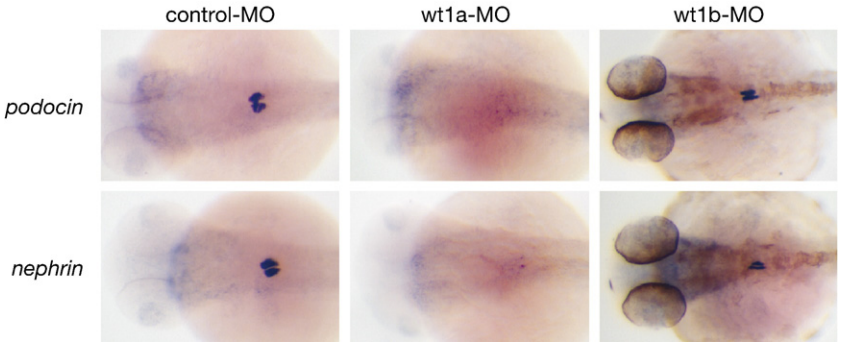

Fig. 4. Differential loss of podocyte-specific marker genes in *wt1a* and *wt1b* morphant embryos. Control, *wt1a* and *wt1b* morpholino-injected embryos were collected at 48 hpf and whole mount *in situ* hybridization was performed using *nephrin* or *podocin* riboprobes. Pigmentation in eyes and trunk of *wt1b* morphants (right panel) is due to pigment cells that escaped PTU treatment.

edema phenotype. *Wt1a* knockdown results in total loss of glomerular differentiation and function and induces severe edema. In contrast, after disruption of *wt1b* mRNA a residual function of the pronephros is maintained leading to a less dramatic kidney phenotype with milder edema.

Discussion

In this work, we have analyzed the function of the Wilms tumor proteins wt1a and wt1b during development of the pronephric kidney in zebrafish. This analysis was possible due to a transgenic line that we had generated for that purpose. Under the assumption that the position of functional elements is roughly conserved between the genome of mammals and fish we cloned a large (25.9 kb) fragment of the zebrafish genome encompassing almost the entire region between *wt1b* and the 5′ lying gene *ga17* and fused it to the *GFP* gene. The resulting transgenic line recapitulated to a large extent the expression pattern of the *wt1b* gene. In addition to the glomeruli, the pronephric tubules as well as the proximal regions of the ducts also showed *GFP* expression. As *wt1b* expression in zebrafish embryos has no yet been observed outside of the glomerulus (Bollig et al., 2006), this might be explained by the expression of very stable GFP mRNA and/or protein in common progenitor cells which give rise to cells of glomeruli, tubules and ducts or by the lack of inhibitory elements on the cloned genomic fragment, which repress *wt1b* expression in tubule and duct cells. Alternatively, the expression of very small amounts of *wt1b* mRNA in the tubules and ducts might have escaped detection by *in situ* hybridization. Nevertheless, because of the expression of *GFP* in glomeruli, tubules and ducts the *wt1b:GFP* line is particularly suited for studies of the entire pronephric kidney.

In the *wt1b:GFP* transgenic embryos *GFP* expression could also be found in the heart sac, eyes and gill arches. This is in agreement with *wt1b* expression in the respective adult tissues (Bollig et al., 2006) and in the developing heart sac. *Wt1* is also expressed in the developing heart and/or heart sac of mice, chicken and frogs (Carmona et al., 2001; Carroll and Vize, 1996; Wagner et al., 2005) and also in the eyes of mouse embryos (Wagner et al., 2002). Thus, the genomic fragment that we have used drives *GFP* expression in many domains that are shared between *wt1b* in zebrafish and *Wt1* in other vertebrates.

As shown previously the two *wt1* paralogs in zebrafish have a similar and overlapping but not identical expression pattern (Bollig et al., 2006). In the intermediate mesoderm, significant *wt1a* expression can be detected earlier (11 hpf) than *w1b* (14 hpf) and in a broader area. At later time points (50 hpf) *wt1b* is expressed more laterally in the glomerulus than *wt1a* and in the area of the glomerular–tubular junction. As anticipated by these expression patterns, we here provide evidence for different functions of *wt1a* and *wt1b* in development of the pronephric kidney in zebrafish. Inactivation of *wt1a* leads to failure of glomerular morphogenesis and differentiation including the absence of podocytes as judged by the lack of respective marker gene expression. This suggests a very early and fundamental role of wt1a in pronephros formation, complying with the earlier and more extended pattern of *wt1a* expression. In contrast, the role of wt1b seems to be required at later stages of pronephric development. This is based on our observation that knockdown of *wt1b* does not interfere with the initial formation of the glomerular structures. Marker gene analysis suggests that in the absence of wt1b differentiation of the podocytes occurs, although at a reduced level. Within the second day of development, however, *wt1b* morphant embryos develop cysts within the glomerular–tubular region of the nephron, which is the region of *wt1b* expression.

To our knowledge this is only the second case where inactivation of Wt1 has been linked to cyst formation. Recently this phenomenon has been described in offspring of *Wt1* knockout mice crossed with mice harboring a *Wt1(−KTS)* transgene (Lahiri et al., 2007). *Wt1* heterozygous animals that carried the transgene showed multiple glomerular cysts. The mechanism by which loss of Wt1 function causes cyst formation is unclear. One possibility is that Wt1 as a transcription factor regulates the expression of podocyte-specific genes like *nephrin* or *podocin*. In fact, Wt1 has been shown to be an activator of *nephrin* in mammals (Guo et al., 2004; Wagner et al., 2004). In zebrafish, it has been reported that inactivation of *nephrin* and *podocin* lead to cysts in the pronephric tubules with a stretched septal glomerulus in the midline (Kramer-Zucker et al., 2005b). Although this phenotype is similar to the one we report here for *wt1b* morphants, the

persistence of *nephrin* and *podocin* expression in these embryos suggests that wt1b must regulate other targets during pronephros development.

It has been shown that cilia-driven fluid flow in the zebrafish pronephros is required for normal organogenesis (Kramer-Zucker et al., 2005a). An intriguing possibility could be that wt1b is involved in the regulation of this fluid flow. It is interesting to note here that disruption of cilia function results in a combination of renal cyst development and body axis curvature (Kramer-Zucker et al., 2005a; Sun et al., 2004). This combination of phenotypic anomalies is also seen in *wt1b* morphant embryos. Whether wt1b might be involved in the regulation of cilia structure or motility is currently under investigation.

The knockdown of wt1a in the *wt1b::GFP* transgenic line was associated with a significant number of cells that were located outside of the area where pronephros development occurred. This effect was specific for *wt1a*, could be observed with both *wt1a* morpholinos and appeared rather early, suggesting that the cells are derived from the pronephric region and not from other expression sites like the exocrine pancreas. It seemed that GFP-positive cells had lost cell–cell contacts and migrated out of the kidney region. The origin of the cells as well as the question whether the cells actively move requires further investigation. In light of the fact that WT1 acts as a tumor suppressor in humans it is tempting to speculate that the loss of cell–cell contacts might contribute to the tumorigenic phenotype of cells with an inactivated *WT1* gene. This could be mediated by the product of the Wt1 target *E-cadherin*, a molecule that increases cell adhesion and decreases invasiveness (Hosono et al., 2000).

It has been shown that the ±KTS isoforms of Wt1 have different functions *in vivo* (Hammes et al., 2001). In zebrafish +KTS and −KTS isoforms can be found for both *wt1* paralogs (Bollig et al., 2006). Given that Wt1 proteins can dimerize (Englert et al., 1995b; Moffett et al., 1995; Reddy et al., 1995), one could speculate that at least in areas of overlapping *wt1a* and *wt1b* expression several different homo- and heterodimers could form. In those cells knockdown of either *wt1a* or *wt1b* could affect functions that are exerted by possible wt1a/wt1b heterodimers. However, our observation concerning the specificity of *wt1a* and *wt1b* knockdown effects would suggest, that those potential heterodimers only play a minor role.

Several lines of evidence suggest that mammalian *Wt1* functions at different sequential steps in metanephric kidney development. Initially, *Wt1* is required for survival of the early metanephric mesenchyme (Kreidberg et al., 1993) and subsequently for nephron formation (Davies et al., 2004). Later on, Wt1 also has a role in glomerular maturation and podocyte function as revealed in human patients with Denys–Drash or Frasier syndrome. How Wt1 acts during these developmental processes is still unclear. There are reports that indicate an apoptosis enhancing function (Englert et al., 1995a; Morrison et al., 2005) for Wt1, others suggest an anti-apoptotic role (Maheswaran et al., 1995; Mayo et al., 1999). In a recent report, an siRNA-based method was used and it was shown that knockdown of *Wt1* in renal organ culture leads to a strong impairment of nephron formation accompanied by increased apoptosis in the organ periphery as well as increased proliferation of cells surrounding the branches of the ureteric buds (Davies et al., 2004). Our data show that although *wt1a* morphant embryos show a loss of GFP-positive nephron structures the number of GFP-positive cells seems to be increased. Moreover, *wt1b* knockdown leads to cyst formation, a process that has recently been shown to be correlated with increased proliferation (Bukanov et al., 2006). Taken together we would speculate that in both *wt1a* and *wt1b* morphants the observed phenotypes are linked to increased cell proliferation rather than to enhanced apoptosis.

The fundamental and early role of wt1a in the development of the zebrafish pronephros is reminiscent of the early function of Wt1 in murine metanephric development. In contrast, wt1b acts at a later stage of pronephros development in zebrafish, namely during nephron differentiation and/or maintenance. It cannot be excluded, however, that wt1a also has a later role in pronephros development and function. Due to the early loss of glomerular structures in *wt1a* morphants possible later roles of wt1a cannot be addressed. From an evolutionary point of view one could speculate that early and late functions in kidney development, which are fulfilled by one *Wt1* gene in mammals are partitioned among two genes in teleost fish. Conditional mouse models that allow us to address potential later roles of *Wt1* will help to address this hypothesis.

Acknowledgments

We thank Nils Hartmann and Jürgen Klattig for discussions and for critically reading and improving this manuscript. We also thank Dirk Meyer for help regarding the characterization of the transgenic line and Christina Ebert for technical support. This work was supported in part by grant En280/7-1 from the Deutsche Forschungsgemeinschaft.

Appendix A. Supplementary data

Supplementary data associated with this article can be found, in the online version, at doi:10.1016/j.ydbio.2007.06.022.

References

Amemiya, C.T., Zon, L.I., 1999. Generation of a zebrafish P1 artificial chromosome library. Genomics 58, 211–213.

Armstrong, J.F., et al., 1993. The expression of the Wilms' tumour gene, WT1, in the developing mammalian embryo. Mech. Dev. 40, 85–97.

Barbaux, S., et al., 1997. Donor splice-site mutations in WT1 are responsible for Frasier syndrome. Nat. Genet. 17, 467–470.

Bollig, F., et al., 2006. Identification and comparative expression analysis of a second wt1 gene in zebrafish. Dev. Dyn. 235, 554–561.

Boute, N., et al., 2000. NPHS2, encoding the glomerular protein podocin, is mutated in autosomal recessive steroid-resistant nephrotic syndrome. Nat. Genet. 24, 349–354.

Bukanov, N.O., et al., 2006. Long-lasting arrest of murine polycystic kidney disease with CDK inhibitor roscovitine. Nature 444, 949–952.

Call, K.M., et al., 1990. Isolation and characterization of a zinc finger polypeptide gene at the human chromosome 11 Wilms' tumor locus. Cell 60, 509–520.

Carmona, R., et al., 2001. Localization of the Wilm's tumour protein WT1 in avian embryos. Cell Tissue Res. 303, 173–186.
Carroll, T.J., Vize, P.D., 1996. Wilms' tumor suppressor gene is involved in the development of disparate kidney forms: evidence from expression in the *Xenopus* pronephros. Dev. Dyn. 206, 131–138.
Davies, J.A., et al., 2004. Development of an siRNA-based method for repressing specific genes in renal organ culture and its use to show that the Wt1 tumour suppressor is required for nephron differentiation. Hum. Mol. Genet. 13, 235–246.
Drummond, I., 2003. Making a zebrafish kidney: a tale of two tubes. Trends Cell Biol. 13, 357–365.
Drummond, I.A., et al., 1998. Early development of the zebrafish pronephros and analysis of mutations affecting pronephric function. Development 125, 4655–4667.
Englert, C., et al., 1995a. WT1 suppresses synthesis of the epidermal growth factor receptor and induces apoptosis. EMBO J. 14, 4662–4675.
Englert, C., et al., 1995b. Truncated WT1 mutants alter the subnuclear localization of the wild-type protein. Proc. Natl. Acad. Sci. U. S. A. 92, 11960–11964.
Gessler, M., et al., 1990. Homozygous deletion in Wilms tumours of a zinc-finger gene identified by chromosome jumping. Nature 343, 774–778.
Guo, J.K., et al., 2002. WT1 is a key regulator of podocyte function: reduced expression levels cause crescentic glomerulonephritis and mesangial sclerosis. Hum. Mol. Genet. 11, 651–659.
Guo, G., et al., 2004. WT1 activates a glomerular-specific enhancer identified from the human nephrin gene. J. Am. Soc. Nephrol. 15, 2851–2856.
Hammes, A., et al., 2001. Two splice variants of the Wilms' tumor 1 gene have distinct functions during sex determination and nephron formation. Cell 106, 319–329.
Hauptmann, G., Gerster, T., 1994. Two-color whole-mount in situ hybridization to vertebrate and Drosophila embryos. Trends Genet. 10, 266.
Holtzinger, A., Evans, T., 2005. Gata4 regulates the formation of multiple organs. Development 132, 4005–4014.
Hosono, S., et al., 2000. E-cadherin is a WT1 target gene. J. Biol. Chem. 275, 10943–10953.
Hsu, H.J., et al., 2003. Parallel early development of zebrafish interrenal glands and pronephros: differential control by wt1 and ff1b. Development 130, 2107–2116.
Huber, T.B., et al., 2003. Molecular basis of the functional podocin-nephrin complex: mutations in the NPHS2 gene disrupt nephrin targeting to lipid raft microdomains. Hum. Mol. Genet. 12, 3397–3405.
Kestila, M., et al., 1998. Positionally cloned gene for a novel glomerular protein—nephrin—is mutated in congenital nephrotic syndrome. Mol. Cell 1, 575–582.
Kimmel, C.B., et al., 1995. Stages of embryonic development of the zebrafish. Dev. Dyn. 203, 253–310.
Klamt, B., et al., 1998. Frasier syndrome is caused by defective alternative splicing of WT1 leading to an altered ratio of WT1 ±KTS splice isoforms. Hum. Mol. Genet. 7, 709–714.
Kramer-Zucker, A.G., et al., 2005a. Cilia-driven fluid flow in the zebrafish pronephros, brain and Kupffer's vesicle is required for normal organogenesis. Development 132, 1907–1921.
Kramer-Zucker, A.G., et al., 2005b. Organization of the pronephric filtration apparatus in zebrafish requires Nephrin, Podocin and the FERM domain protein Mosaic eyes. Dev. Biol. 285, 316–329.
Kreidberg, J.A., et al., 1993. WT-1 is required for early kidney development. Cell 74, 679–691.
Lahiri, D., et al., 2007. Nephropathy and defective spermatogenesis in mice transgenic for a single isoform of the Wilms' tumour suppressor protein, WT1-KTS, together with one disrupted Wt1 Allele. Mol. Reprod. Dev. 74, 300–311.
Lang, M.R., et al., 2006. Secretory COPII coat component Sec23a is essential for craniofacial chondrocyte maturation. Nat. Genet. 38, 1198–1203.
Livak, K.J., Schmittgen, T.D., 2001. Analysis of relative gene expression data using real-time quantitative PCR and the 2(−Delta Delta C(T)) method. Methods 25, 402–408.
Maheswaran, S., et al., 1995. The WT1 gene product stabilizes p53 and inhibits p53-mediated apoptosis. Genes Dev. 9, 2143–2156.
Majumdar, A., et al., 2000. Zebrafish no isthmus reveals a role for pax2.1 in tubule differentiation and patterning events in the pronephric primordia. Development 127, 2089–2098.
Mayo, M.W., et al., 1999. WT1 modulates apoptosis by transcriptionally upregulating the bcl-2 proto-oncogene. EMBO J. 18, 3990–4003.
McCune, A.R., Carlson, R.L., 2004. Twenty ways to lose your bladder: common natural mutants in zebrafish and widespread convergence of swim bladder loss among teleost fishes. Evol. Dev. 6, 246–259.
Moffett, P., et al., 1995. Antagonism of WT1 activity by protein self-association. Proc. Natl. Acad. Sci. U. S. A. 92, 11105–11109.
Moore, A.W., et al., 1998. YAC transgenic analysis reveals Wilms' tumour 1 gene activity in the proliferating coelomic epithelium, developing diaphragm and limb. Mech. Dev. 79, 169–184.
Morrison, D.J., et al., 2005. WT1 induces apoptosis through transcriptional regulation of the proapoptotic Bcl-2 family member Bak. Cancer Res. 65, 8174–8182.
Palmer, R.E., et al., 2001. WT1 regulates the expression of the major glomerular podocyte membrane protein Podocalyxin. Curr. Biol. 11, 1805–1809.
Pavenstadt, H., et al., 2003. Cell biology of the glomerular podocyte. Physiol. Rev. 83, 253–307.
Pelletier, J., et al., 1991. Germline mutations in the Wilms' tumor suppressor gene are associated with abnormal urogenital development in Denys–Drash syndrome. Cell 67, 437–447.
Pritchard-Jones, K., et al., 1990. The candidate Wilms' tumour gene is involved in genitourinary development. Nature 346, 194–197.
Rackley, R.R., et al., 1993. Expression of the Wilms' tumor suppressor gene WT1 during mouse embryogenesis. Cell Growth Differ. 4, 1023–1031.
Reddy, J.C., et al., 1995. WT1-mediated transcriptional activation is inhibited by dominant negative mutant proteins. J. Biol. Chem. 270, 10878–10884.
Riccardi, V.M., et al., 1978. Chromosomal imbalance in the Aniridia–Wilms' tumor association: 11p interstitial deletion. Pediatrics 61, 604–610.
Rivera, M.N., Haber, D.A., 2005. Wilms' tumour: connecting tumorigenesis and organ development in the kidney. Nat. Rev., Cancer 5, 699–712.
Roselli, S., et al., 2004. Plasma membrane targeting of podocin through the classical exocytic pathway: effect of NPHS2 mutations. Traffic 5, 37–44.
Sun, Z., et al., 2004. A genetic screen in zebrafish identifies cilia genes as a principal cause of cystic kidney. Development 131, 4085–4093.
Thermes, V., et al., 2002. I-*Sce*I meganuclease mediates highly efficient transgenesis in fish. Mech. Dev. 118, 91–98.
Wagner, K.D., et al., 2002. The Wilms' tumor gene Wt1 is required for normal development of the retina. EMBO J. 21, 1398–1405.
Wagner, N., et al., 2004. The major podocyte protein nephrin is transcriptionally activated by the Wilms' tumor suppressor WT1. J. Am. Soc. Nephrol. 15, 3044–3051.
Wagner, N., et al., 2005. Coronary vessel development requires activation of the TrkB neurotrophin receptor by the Wilms' tumor transcription factor Wt1. Genes Dev. 19, 2631–2642.